Modeling Water and Heat Balance of the Boreal Landscape—Comparison of Forest and Arable Land in Scandinavia

DAVID GUSTAFSSON

WSL, Swiss Federal Institute for Snow and Avalanche Research, Davos, Switzerland, and Department of Land and Water Resources Engineering, Royal Institute of Technology, Stockholm, Sweden

ELISABET LEWAN

Division of Environmental Physics, Department of Soil Sciences, Swedish University of Agricultural Sciences, Uppsala, Sweden

PER-ERIK JANSSON

Department of Land and Water Resources Engineering, Royal Institute of Technology, Stockholm, Sweden

(Manuscript received 25 June 2003, in final form 28 May 2004)

ABSTRACT

The water and heat balances of an arable field and a forest in the boreal zone in Scandinavia were explored using 3 yr of observations and simulations with two different soil–vegetation–atmosphere transfer (SVAT) models over a 30-yr period. Results from a detailed mechanistic model [coupled heat and mass transfer model (COUP)] were compared with those obtained with a large-scale type of SVAT model used in the weather prediction model at the European Centre for Medium-Range Weather Forecasts [ECMWF tiled land surface scheme (TESSEL)]. The COUP model simulations agreed well with the observations from a seasonal perspective. The TESSEL model differed significantly from the measurements when standard operational parameter values were used. The introduction of a seasonal variation in leaf-area index values, tuned canopy resistance for forest, and a reduced roughness length over snow-covered open land reduced the discrepancies. Net radiation was 40% higher in the forest when compared with the arable land, based on 30-yr simulations with both models. Furthermore, the forest was a net source of sensible heat flux, whereas the arable land was a net sink. Because of different treatment of winter interception evaporation, forest latent heat flux based on the COUP model considerably exceeded that from the TESSEL model, and suggested that the total annual evaporation was higher from the forest than from arable land. The representation of interception evaporation in winter, as well as seasonal dynamics in vegetation properties are, thus, of considerable importance for adequate simulation of forest and arable land energy fluxes within the boreal zone.

1. Introduction

Land surface heat exchange processes are important boundary conditions for atmospheric processes as well as for hydrological, biological, and chemical processes at the land surface. Processes at the land surface govern the input of heat and moisture to the atmosphere by the absorption of solar radiation and the partitioning of net radiation (R_n) into sensible (H) and latent heat (LE). Land surface heat exchange also governs the soil microclimate and, thus, the storage and release of carbon, methane, and other greenhouse gases, which have a long-term effect on the climate.

This study focused on the land surface exchange processes in the boreal zone in northern high latitudes. This is a region where climate change due to increased atmospheric CO_2 will be most pronounced according to general circulation model (GCM) predictions (Houghton et al. 1996). The boreal zone is dominated by evergreen forests, with open areas of lakes, bogs, and arable fields spread out in a mosaic pattern. Several GCM studies have shown that the boreal forests have a significant impact on the climate of the Northern Hemisphere (Thomas and Rowntree 1992; Bonan et al. 1995; Douville and Royer 1997). Forests contribute more heat and moisture to the atmosphere compared to open areas with low vegetation, such as tundra or grassland meadows. This is thought to be a consequence of the higher input of net radiation to the forest, especially in winter when the high albedo of the snow is overshadowed by the low albedo of the trees. In dry summer conditions, evapotranspiration may be higher from open areas than from forests, because of the typically higher transpira-

Corresponding author address: David Gustafsson, Department of Land and Water Resources Engineering, Royal Institute of Technology KTH, SE-100 44 Stockholm, Sweden.
E-mail: davidg@kth.se

tion by, for example, grassland and arable crops than by evergreen forest trees. However, higher rates of interception evaporation in forests, especially in winter, may contribute to a higher total evapotranspiration from forests averaged over the year.

To understand the complex interactions within a mixed landscape of different land cover and land use, improved understanding of the component land units is also required. It is, therefore, of significant interest to further evaluate and quantify differences in the exchange of water and heat between different surface types within the boreal landscape. Bringfelt et al. (1999) compared the water and heat exchange above neighboring experimental sites in forests, arable fields, and a lake in the Scandinavian boreal zone. For a single summer day they found that the Bowen ratio ($\beta = H/\mathrm{LE}$) was 1–3 above forest areas, less than 1 above arable fields, and around 0 above the lake. Midday sensible heat flux varied from approximately 300 above the forest to 100 W m^{-2} above the arable fields and to just below zero above the lake. Observed latent heat fluxes were in the range of 100–250 W m^{-2} above both the forest and arable land, but not more than 100 W m^{-2} above the lake. In a similar study in winter, Harding and Pomeroy (1996) showed that during the snowmelt season, a snow-covered lake was a net sink for sensible heat flux, at the same time as a nearby forest was a net source of sensible heat flux. It has also been shown that the evaporation of intercepted rain or snow has a greater effect on the surface energy balance and hydrology of forests compared to open land. The accumulated snow on the ground may be reduced by up to 30% in forests because of the evaporation of intercepted snow (Harding and Pomeroy 1996). On the other hand, snowmelt rates can be lower in forests because of the reduced radiation and turbulent exchange below the canopy (Ohta et al. 1993).

Models describing the water and heat exchange in the soil–vegetation–atmosphere system are important components in weather prediction and climate models. Soil–vegetation–atmosphere transfer (SVAT) models are also tools for analyses of the impact of different land use on water and land resources. The SVAT models differ depending on their origin and the main purpose for which they have been developed. Typical differences are related to the scale and the degree of aggregation of different components. The need for evaluation and adequate parameterization of SVAT models with respect to different terrestrial ecosystems has been stressed in order to reduce the uncertainties in GCM predictions (Viterbo and Beljaars 1995; Henderson-Sellers 1996; Chen et al. 1997; Verseghy 2000). Several large-scale projects have been established to investigate land surface exchange processes in different climate regions and ecosystems. The Boreal Ecosystem–Atmosphere Study (BOREAS; Sellers et al. 1997) and Northern Hemisphere Climate Processes Land-Surface Experiment (NOPEX; Halldin et al. 1998) projects have contributed valuable knowledge of boreal ecosystems in Canada and Scandinavia, respectively.

The objectives of this study were 1) to compare the seasonal water and heat balances of a forest and an open arable field at the southern edge of the Scandinavian boreal zone as represented by observations and site-specific model simulations, and 2) to evaluate the current representation of these types of land covers within the boreal zone in a typical large-scale GCM model. A detailed SVAT model [coupled heat and mass transfer model (COUP); Jansson and Karlberg 2001] was used to explain general differences in seasonal dynamics and long-term budgets of water and heat flux components of the two surfaces. The model has been developed from a hydrological local-scale perspective and represents a ''mixed vegetation–cover approach'' where the land surface is represented by a number of vertically stratified and interacting subsurfaces (e.g., bare soil, snow, vegetation, intercepted water). The results from this model were compared with those obtained from an SVAT model used in operational weather forecasts [European Centre for Medium-Range Weather Forecasts (ECMWF) tiled land surface scheme (TESSEL); van den Hurk et al. 2000]. The TESSEL model represents a ''mosaic vegetation–cover approach'' where the land surface is represented by independent subsurfaces scaled by their areal fractions (Koster and Suarez 1992).

The COUP model was parameterized based on site-specific measurements in a forest and at an open arable field within the NOPEX area, whereas the TESSEL model was parameterized for each land cover type that was used in its operational version with only minor site-specific modifications. Both models were evaluated with 3 yr of observations from the field and the forest sites. Based on these results, the TESSEL model was also applied with a tuned parameterization including seasonal variation in vegetation properties (TESSEL*). Each model was run with 30-yr driving datasets for forest and open arable land. The results were compared with respect to the average seasonal variation in water and heat flux components for both land covers.

2. Materials and methods

a. Field sites and data

The central NOPEX experimental site on the Norunda Common (60°5′N, 17°29′E; altitude 45 m), hereinafter referred to as the Norunda forest site, is located about 30 km north of Uppsala, Sweden. The region is flat, and the central tower site has a maximum fetch of 6 km and a minimum fetch of 1 km. The surrounding area consists of 70–100-yr-old forest dominated by Norway spruce and Scots pine of a rather uniform height (25–30 m) and leaf-area index (3–5 m^2 m^{-2}). The soil type is a deep, boulder-rich sandy till of glacial origin.

A continuous climate-monitoring program has been running at the site since June 1994. Turbulent fluxes of

sensible and latent heat, shortwave and longwave radiation, and meteorological variables were measured on the 102-m mast at the center of the site. Soil moisture, soil temperature, soil heat flux, and stem sap flow were measured in the surrounding forest stands as described by Lundin et al. (1999). A 3-yr dataset was available for this study, including meteorological forcing from 1 January 1994 to 31 December 1996 and validation variables from 1 June 1994 to 31 October 1996 (Gustafsson et al. 2003), as summarized in Table 1. The average closure in the present dataset was estimated at 86% (96% in summer; Grelle 1997; Gustafsson et al. 2003) based on net radiation, eddy-correlation fluxes, and soil surface heat flux. The accuracy of the eddy-correlation measurements was estimated at 1.8% and 7.3% for sensible and latent heat flux, respectively (Grelle 1997). One uncertainty related to the estimated energy balance closure is that the net radiation represents a relatively small area around the mast, whereas the eddy-correlation measurements may have a source area ranging from less than 50 m to several kilometers from the mast (Grelle 1997). Second, the heat storage within the canopy was not taken into account.

The agricultural field site at the Marsta Meteorological Observatory (59°55′N, 17°35′E) is located about 9 km north of Uppsala and is hereinafter referred to as the Marsta field site. The site is located in a flat agricultural area, with an open fetch of about 0.5–4 km, limited by small forest areas. The soil type is loamy clay with an organic content of 6% in the topsoil and 2.5% in the subsoil. The management of the surrounding fields is typical for the area, the growing season normally starts in May and harvest takes place in August. The fields are ploughed in autumn and sown with either winter or spring crops, or left uncultivated during the winter and the following summer (fallow; Halldin et al. 1999). A dataset, including meteorological forcing variables and validation variables of surface heat fluxes, as well as snow and soil physical conditions, was put together within the ''WINTEX'' project (the wintertime extension of the NOPEX project), as described in Halldin et al. (1999) and Gustafsson et al. (2001; Table 1). The dataset covers nearly 3 yr from 1 November 1997 to 31 July 2000. Turbulent fluxes of sensible and latent heat above the arable field were measured with eddy correlation on a 3.5-m mast. Soil temperature and soil moisture content were measured in four soil profiles in an arable field located in the prevailing wind direction (southwest) for the eddy flux measurements. Net radiation and its upward and downward components were measured above a short-cut lawn within the observatory area. Unfortunately there were no measurements of the net radiation or any of its components available for the agricultural fields. Snow depth was measured continuously at one point close to the soil profiles and manually once a week along a 75-m transect. Latent heat flux was systematically underestimated by the eddy-correlation system at Marsta, because the frequency resolution of

TABLE 1. Validation variables at the Norunda forest site and the Marsta arable field site.

Variable	Location: Norunda	Location: Marsta	Instrument
Latent heat flux (W m^{-2})	35 m[a]	3.5 m[b]	Sonic anemometer (Solent Basic, Gill Instruments; Lymington, United Kingdom) and gas analyzer (LI-6262; LI-COR, Lincoln, NE)
Sensible heat flux (W m^{-2})	35 m[a]	3.5 m[b]	Sonic anemometer (as above)
Net radiation (W m^{-2})	68 m (96%), 98 m (4%)[c]	1.5 m[d]	Net radiometer (LXV055; Dr. Bruno Lange, Berlin, Germany)
Soil heat flux (W m^{-2})	6-cm depth[e]	Not measured	Heat-flux plates (HFT-1; REBS, Seattle, WA)
Tree sap flow (mm day^{-1})	Trees within 30 m from the central tower[f]	Not measured	Tissue heat balance sap flow meter (P609.2, Environmental Measuring Systems, Brno, Czech Republic)
Soil temperature (°C)	6 levels: 0–100 cm[e]	8 levels: 0–100 cm[b]	Thermocouple (In Situ; Ockelbo, Sweden)
Soil moisture (m^3 m^{-3})	6 levels: 0–100 cm[e]	5 levels: 0–100 cm[b]	Time domain reflectivity (1502B; Tektronix, Pittsfield, MA)

[a] Grelle and Lindroth (1996); Grelle et al. (1999).
[b] Jansson et al. (2001).
[c] Mölder at al. (1999b).
[d] Halldin (2001).
[e] Kellner et al. (1999).
[f] Cienciala et al. (1999).

the gas analyzer was too low (Gustafsson et al. 2001; Gustafsson 2002). The observed sensible heat flux was of similar accuracy as for the forest site.

Four 30-yr meteorological datasets representing forest and arable land at Norunda and Marsta were constructed from observations at Uppsala Airport from 1970 to 1999. Observations of air temperature, wind speed, and humidity at Uppsala Airport were interpolated to the Marsta and Norunda sites using linear regression functions based on overlapping time periods. The interpolation of precipitation to the Norunda site was uncertain, because only summertime observations were available from Norunda. A constant correction of +10% was added to the precipitation data from Uppsala Airport, based on the ratio of accumulated summertime precipitation at the two sites. The forest and the arable land datasets were assumed to differ only with respect to wind speed, which was obtained from correlations with the observed wind speed at the Norunda forest and the Marsta arable land, respectively.

b. Model descriptions

The models have been described in detail in previous papers and only a short summary is given below. The COUP model was first presented as the ''SOIL'' model (Jansson and Halldin 1979). The most recent technical description of the model can be downloaded from the Internet (found online at http://www.lwr.kth.se/Vara%20Datorprogram/CoupModel/index.htm). Previous applications of the model in the NOPEX region have been reported by Jansson et al. (1999) for the forest stand and by Johnsson and Jansson (1991), Gustafsson et al. (2001), and Gustafsson (2002) for the arable land. The TESSEL model (van den Hurk et al. 2000) is the latest version of the land surface scheme in the general circulation model used for weather predictions at ECMWF, (Reading, United Kingdom). The model has been designed to describe the land surface heat exchange processes of a GCM grid cell at a horizontal scale of 50–100 km. Different versions of the land surface scheme were tested and evaluated for the NOPEX forest as reported by Gustafsson et al. (2003).

1) BASIC MODEL STRUCTURES

Both models are based on the energy balance approach (i.e., the net radiation is partitioned into latent and sensible heat and a possible storage term), and simulate the water and heat balance of a vertical soil profile discretized into horizontal layers. Water and heat exchange between the soil and the atmosphere are estimated from similar types of surface compartments—bare soil, snow, vegetation, and intercepted precipitation. The main conceptual differences between the models concern the spatial configuration of, and interaction between, the surface compartments. The COUP model is based on a vertical structure of the surface compartments and allows for simultaneous water and heat exchange from the vegetation layer and soil/snow surface below. The soil surface constitutes the upper boundary for the soil profile, and exchanges of heat and water take place through the snowpack and/or the canopy above. The partitioning of net radiation and precipitation between the vegetation layer and the surfaces below is governed by classical interception concepts. In the TESSEL model, surface compartments represent specific areal fractions, which are linked to the soil and to the atmosphere independently of each other. The surface compartments are referred to as tiles, because they are tiled side by side. This procedure allows for an efficient computation scheme, which is preferable in a GCM model structure. A specific tile is also defined to represent the occurrence of snow below high vegetation. Other model differences are related to the numerical procedures and the degree of detail in the description of different processes, which is further discussed below.

2) SOLUTION OF ENERGY BALANCE EQUATIONS FOR DIFFERENT SURFACES

The TESSEL model uses the same approach to solve the energy balance equation for each surface type (bare soil, low vegetation, high vegetation, intercepted water, snow on low vegetation, and high vegetation with snow beneath). Surface heat fluxes of the individual tiles are estimated with a numerical procedure that accounts for the feedback of the surface temperatures on both net radiation and resistances.

The COUP model uses different numerical methods for different surface types. The dynamic coupling between surface temperature and heat fluxes, which is used in the TESSEL model, is only used for the bare soil surface and for the snow surface. Evaporation from the vegetation, that is, transpiration and evaporation of intercepted water, is calculated with the analytical approach suggested by Penman (1953) as modified by Monteith (1965). The sensible heat flux and the corresponding surface temperature of the vegetation are calculated based on the residual term of the energy balance for the vegetation.

3) INTERCEPTION OF PRECIPITATION

Interception and evaporation of intercepted water in both liquid and frozen forms are accounted for in the COUP model. Transpiration or interception is excluded only when the snow depth exceeds the height of the vegetation layer. Dewfall is considered whenever the potential evaporation is negative. The ratio between the evaporation from intercepted water and transpiration is estimated as the ratio between the corresponding potential rates. Interception of rain or snow on the canopy occurs as long as the precipitation is below the interception capacity, which is assumed to be higher for snow than for rain. The TESSEL model only accounts for

interception processes in snow-free conditions. Fractional surface cover of the intercepted water is assumed to equal the ratio between the interception storage and the interception capacity and thus changes dynamically for both the high and low vegetation tiles in proportion to the interception storage.

4) CONTROL OF TRANSPIRATION

Both models account for the regulation of canopy resistance by shortwave radiation and atmospheric vapor pressure deficit. The transpiration is also governed by soil moisture conditions as reduced below prescribed soil moisture threshold values. However, the COUP model allows for a flexible distribution of the root water uptake in the soil profile under limiting soil water conditions. Soil frost reduces transpiration in both models as a result of reduced liquid soil moisture content, but in the COUP model transpiration is also controlled by the soil temperature under unfrozen soil conditions.

c. Model parameterization

1) PARAMETERIZATION STRATEGY

The COUP model parameter values for the forest and arable land (Table 2) were partly adopted from previous applications of the model to the Norunda forest (Jansson et al. 1999) and the Marsta arable land (Gustafsson et al. 2001; Gustafsson 2002). These parameterizations were based on literature values, site-specific estimates, and calibrations against the available observations of surface heat fluxes, net radiation, surface albedo, soil temperature, and liquid soil moisture content. A reparameterization of the forest in the COUP model, concerning a few winter-related processes, was required compared to Jansson et al. (1999), due to recent model developments and the extension into winter periods (Table 2). The TESSEL model was parameterized for the forest and the arable land in two different ways: (a) with the default parameter values for boreal forest and open land used within the operational version for the closest grid point (van den Hurk et al. 2000), here denoted ''TESSEL,'' and (b) with tuned parameter values for leaf-area index and minimum canopy resistance for both surface types, and for roughness length over snow-covered open land ''TESSEL*.'' The more important differences between the COUP and TESSEL model parameterizations are discussed below.

2) SOIL PROFILE AND SOIL PHYSICAL PROPERTIES

A 12-m-deep soil profile was used in the COUP model simulations, in order to minimize the influence of the lower boundary conditions for heat flow. Soil physical properties were based on site-specific soil core samples taken down to a depth of 1 m at the Norunda and the Marsta sites, respectively (Stähli et al. 1995; Gustafsson et al. 2001). The thermal conductivity of the forest soil surface was selected to represent an organic layer of 2-cm depth following de Vries (1975), approximately 90% lower than for the mineral soil below.

The TESSEL model was parameterized according to the operational model version with four soil layers with total thickness of 2.89 m. Soil physical properties are vertically uniform and are based on an average of the medium-textured soils in the U.S. Department of Agriculture soil classification (Viterbo and Beljaars 1995). The properties of this soil represent an intermediate compared to the hydraulic properties estimated for the Marsta and the Norunda sites (Table 2).

3) FOREST SURFACE PROPERTIES

The COUP model parameters governing the canopy surface resistance, actual root water uptake, and within-canopy aerodynamic resistances for interception evaporation, snow evaporation, and bare soil evaporation were all chosen according to Jansson et al. (1999). However, a maximum upper limit of the aerodynamic resistance set to 500 s m^{-1} was needed to avoid unrealistically low canopy surface temperatures. A seasonal variation in leaf-area index (LAI) of 10% around the mean value (4.5 m^2 m^{-2}) was used, based on a sensitivity analysis with the TESSEL model by Gustafsson et al. (2003).

The forest parameters in the TESSEL model were based on the values used for the closest grid point in the operational model (van den Hurk et al. 2000), except for some site-specific parameters. The fractional surface coverage of the vegetation was set to 90% in the TESSEL model, partitioned on 98% high vegetation and 2% low vegetation (Gustafsson et al. 2003). Aerodynamic properties (Mölder et al. 1999a) and surface albedo of the vegetation (Mölder et al. 1999b) were taken from site-specific estimations for both models. In the second application, the TESSEL model was run with the same seasonal variation in forest LAI as applied in the COUP model (TESSEL*, Table 2), and with a 25% reduction of the minimum canopy resistance for transpiration.

4) ARABLE LAND SURFACE PROPERTIES

The COUP model was parameterized based on calibrations with the Marsta data (Gustafsson 2002). To obtain a reasonable simulation of the surface heat fluxes, a seasonal development of leaf-area index and canopy height, and a smaller roughness length for snow-covered conditions had to be used. An average vegetation for the area was represented by a start of the growing season on 1 May, a maximum leaf-area index (4 m^2 m^{-2}), a maximum canopy height (1.0 m) on 1 July, and harvest on 1 September based on Persson (1997) and Halldin et al. (1999). Surface canopy cover was estimated as a function of LAI, with the maximum areal fraction set to 0.9.

TABLE 2. Parameter values used in the COUP and the TESSEL model simulations of the Norunda forest and the Marsta field. Parameter values for the TESSEL model were approximated corresponding to the definition of the parameters in the COUP model.

Parameter	COUP Forest	Arable land	TESSEL Forest	Arable land
Radiation properties				
Albedo of vegetation and soil (%)	8.15–9.65[a]	19–25[b]	8.15–9.65[a]	19–25[b]
Fraction of net radiation absorbed by canopy	0.91–0.95[c]	0.16–0.91[d]	0.97[e]	0.97[e]
Albedo of snow (%)	65–40[f]	85–40[b]	15[e]	85–40[e]
Vegetation properties				
Leaf-area index ($m^2\ m^{-2}$)	4.05–4.95[a]	0.3–4[g]	4.5,[a,h] 4.05–4.95[a]	3,[a,h] 0.3–4[g]
Canopy height (m)	27.5[i]	0.1–1.0[g]	Not defined	Not defined
Canopy surface cover ($m^2\ m^{-2}$)	1[c]	0.3–0.9[j]	0.9[a]	0.9; 0.3–0.9[j]
Potential transpiration				
Half radiation saturation ($W\ m^{-2}$)	130[f]	130[f]	149[e]	149[e]
Vapor pressure (Pa)	359[c]	200[k]	2310[e]	2310[e]
Maximal conductance ($m\ s^{-1}\ LAI^{-1}$)	0.005[c]	0.02[k]	0.0027,[e,h] 0.0036[a]	0.006[e]
Aerodynamic properties				
Displacement height (m)	21.1[l]	0–0.66[m]	21.1[l]	0[e]
Roughness length momentum z_{0M} (m)	1.75[l]	0.01–0.1[b]	1.75[l]	0.1,[e,h] 0.01–0.1[b]
Roughness length heat z_{0H} (m)	1/10 of z_{0M}^{e}	1/10 of z_{0M}^{e}	1/10 of z_{0M}^{e}	1/10 of z_{0M}^{e}
Increase of aerodynamic resistance below canopy ($s\ m^{-1}$)	400–500[c]	30–400[b]	100[e]	Not defined
Water uptake				
Root depth (m)	0.7[c]	1[b]	2.89[e]	1[e]
Critical threshold for reduction (vol % and cm tension)	11.9%–28.1% −150 cm[c]	23.7%–32.1% −3000 cm[b]	32.3% −342 cm[e]	32.3% −342 cm[e]
Flexibility degree	0.7[e]	0.7[b]	0[e]	0[e]
Interception				
Interception capacity ($mm\ LAI^{-1}$)	0.3 (rain)[c] 5.9 (snow)[m]	0.2 (rain)[e]	0.2[e]	0.2[e]
Within-canopy resistance ($s\ m^{-1}\ LAI^{-1}$)	5 (rain)[c] 50 (snow)[n]	10[c]	0[e]	0[e]
Interception efficiency	0.6[o]	0.5[c]	0.5[e]	0.5[e]
Hydraulic properties				
Soil porosity (vol %)	45.3–55.8[c]	46–62.4[b]	47.2[e]	47.2[e]
Air entry pressure (cm)	3.2–14.9[c]	0.2–2.2[b]	34.6[e]	34.6[e]
Pore size distribution index	0.16–0.39[c]	0.05–0.12[b]	0.17[e]	0.17[e]
Water content wilting point (vol %)	3.4–6.4[c]	15.6–20.6[b]	17.1[e]	17.1[e]
Hydraulic conductivity at saturation ($m\ s^{-1}$)	$>8.10 \times 10^{-7}$ $<1.25 \times 10^{-4}$[c]	$>1.05 \times 10^{-4}$ $<1.27 \times 10^{-5}$[b]	4.57×10^{-6}[e]	4.57×10^{-6}[e]

[a] Gustafsson et al. (2003).
[b] Gustafsson (2002).
[c] Jansson et al. (1999).
[d] Barfield et al. (1973.
[e] van den Hurk et al. (2000).
[f] Calibration.
[g] Persson (1997).
[h] Modified versions of the TESSEL model, according to this paper.
[i] Lundin et al. (1999).
[j] Assumed.
[k] Heidmann et al. (2000).
[l] Mölder et al. (1999a).
[m] Hedstrom and Pomeroy (1998).
[n] Koivusalo and Kokkonen (2002).
[o] Lankreijer et al. (1999).

The TESSEL model was parameterized according to the default parameter set used for open land in the operational version (van den Hurk et al. 2000). This implies a constant LAI (=3) and a fixed roughness length (0.1 m) throughout the year. In the second application (TESSEL*) the TESSEL model was run with slight modifications: a seasonal variation in LAI (as in the COUP model) and the roughness length over snow-covered areas reduced by one order of magnitude (Table 2).

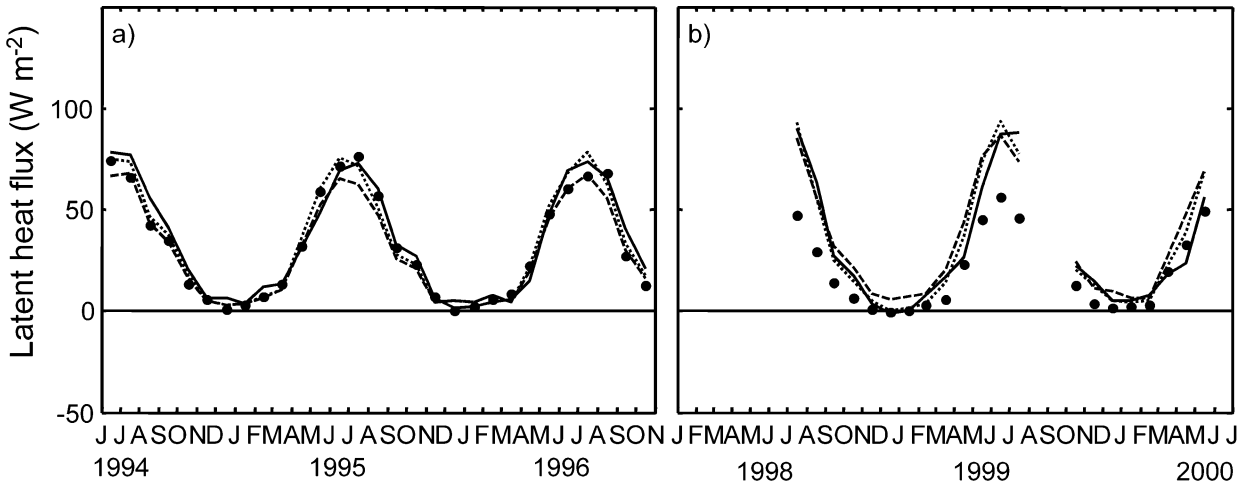

FIG. 1. Latent heat flux for (a) Norunda forest 1994–96 and (b) Marsta arable land 1997–2000, monthly averages, measurements (crosses), and simulations with the COUP (solid line), the TESSEL (dashed line), and the TESSEL* (dotted line) models.

d. Model applications

1) MODEL EVALUATION

Both models were run with hourly meteorological data and were evaluated based on the 3-yr datasets from Norunda (January 1994–December 1996) and Marsta (November 1997–July 2000). Initial values were obtained by simulating the three preceding years before the evaluation periods, starting with climatological soil temperature profiles derived from average annual air temperature variations, and soil moisture content representing field capacity.

Daily average values of observed latent heat flux, sensible heat flux, net radiation, soil temperatures, soil moisture storage, transpiration, and surface albedo were used as validation data. For the Marsta site, less emphasis was placed on the comparison with observed latent heat flux because of the systematic underestimation in the measurements. The ability of the models to reproduce the observations from forest and arable land was evaluated based on 1) the coefficient of determination (r^2), intercept (a_0), and slope (a_1) obtained by the linear regression of simulated versus observed values, 2) mean error (ME), and 3) root-mean-square error (rmse).

2) 30-YEAR SIMULATIONS

The COUP and the TESSEL models were run with the 30-yr driving datasets for forest and arable land as constructed for both Marsta and Norunda. In order to verify whether the parameterizations were independent of the meteorological forcing, both datasets were used for simulations with the forest and the arable land parameterizations. Annual average courses and budgets of surface heat fluxes, net radiation, soil temperatures, and soil moisture storage were compared. It was found that the differences between the forest and the arable land simulations were similar irrespective of whether the Norunda or the Marsta driving data were used. Therefore, only the result from simulations with forcing datasets for one of the sites (Marsta) was used for further analyses. To minimize the influence of initial conditions, the first 5 yr of the simulations were excluded from the analyses.

3. Results and discussion

a. Comparison of simulations and measurements

1) NORUNDA FOREST, 1994–96

Both COUP and TESSEL reproduced fairly well the observed seasonal variation in latent and sensible heat flux from the forest site (Figs. 1a and 2a). Nevertheless, the models differed systematically from each other and from the measurements in some critical aspects. Generally, the latent heat flux was best reproduced by the tuned version of the TESSEL model (TESSEL*), whereas the sensible heat flux was better reproduced by COUP (Tables 3 and 4).

The interannual variation in summer latent heat flux was unsatisfactorily described by all models. TESSEL* agreed best with observations in 1994, whereas COUP was closest in 1995 and the original TESSEL model in 1996 (Fig. 1a). The introduction of a seasonal variation in LAI and a reduced minimum canopy resistance in the TESSEL model improved the simulated latent heat flux in summer 1994 and 1995, but not for 1996 (Fig. 1a). Both models also underestimated transpiration compared to observations in late summer 1995 and 1996 (data not shown). This indicates that seasonal variation in vegetation properties were of significant importance for the description of seasonal latent heat flux at this site, but also that an interannual variation in vegetation properties may be needed to further improve the result. Both COUP and TESSEL* agreed well with the evap-

TABLE 3. Simulated values vs observations, Norunda, summer days (May–Oct) 1994–96, based on daily averages. TESSEL* is the modified version adopted to the Norunda site, including seasonal variation in leaf-area index and reduction of minimum canopy resistance for high vegetation to 75% of its original value.

Variable	r^2	a_0	a_1	ME	Rmse	N
LE (W m^{-2})						
COUP	0.76	13.87	0.79	3.50	13.38	442
TESSEL	0.76	7.56	0.77	−3.53	13.34	442
TESSEL*	0.77	6.81	0.90	2.04	13.46	442
H (W m^{-2})						
COUP	0.90	7.09	0.79	0.24	17.69	442
TESSEL	0.88	16.98	0.72	7.77	21.82	442
TESSEL*	0.87	13.47	0.67	2.67	22.17	442
R_n (W m^{-2})						
COUP	1.00	−0.60	0.97	−3.42	4.89	442
TESSEL	1.00	0.15	0.98	−1.28	3.10	442
TESSEL*	1.00	0.30	0.99	−0.79	2.93	442
T 7–21 cm (°C)						
COUP	0.97	−0.96	1.16	0.57	0.95	511
TESSEL	0.93	−2.50	1.44	1.78	2.52	511
TESSEL*	0.93	−2.55	1.43	1.71	2.46	511
Transpiration (mm day^{-1})						
COUP	0.87	0.32	0.79	0.10	0.37	444
TESSEL	0.86	0.21	0.71	−0.09	0.39	444
TESSEL*	0.86	0.25	0.87	0.11	0.37	444

oration components estimated for the Norunda forest from 16 May to 31 October 1995 by Grelle et al. (1997), although both models underestimated the measured transpiration (Table 5). The COUP model was in best agreement with the observed interception evaporation.

Wintertime latent heat flux was slightly overestimated by the COUP model in 1994–95 and by the TESSEL models in 1995–96 (Fig. 1a). These overestimations were related to snow evaporation in both models. However, in the COUP model it originated from intercepted snow, whereas in the TESSEL models (which do not consider snow interception) from snow below the forest canopy. The discrepancies between observed and simulated wintertime latent heat fluxes were relatively

TABLE 4. Simulated values vs observations, Norunda, winter days (Nov–Apr) 1994–96, based on daily averages. TESSEL* is the modified version adopted to the Norunda site, including seasonal variation in leaf area index and reduction of minimum canopy resistance for high vegetation to 75% of its original value.

Variable	r^2	a_0	a_1	ME	Rmse	N
LE (W m^{-2})						
COUP	0.60	2.66	0.66	−0.06	7.61	316
TESSEL	0.56	2.58	0.67	−0.11	8.02	316
TESSEL*	0.58	2.47	0.74	0.40	8.09	316
H (W m^{-2})						
COUP	0.78	−3.81	0.82	−2.29	16.50	316
TESSEL	0.72	3.79	0.73	6.11	19.51	316
TESSEL*	0.71	3.20	0.71	5.66	19.69	316
R_n (W m^{-2})						
COUP	0.97	−3.33	0.92	−3.57	8.28	316
TESSEL	0.97	0.09	0.97	−0.01	6.97	316
TESSEL*	0.97	0.14	0.97	0.05	6.97	316
T 7–21 cm (°C)						
COUP	0.94	0.13	0.89	0.00	0.42	421
TESSEL	0.74	−2.19	1.27	−1.88	2.35	421
TESSEL*	0.93	−2.55	1.43	1.71	2.46	511
Transpiration (mm day^{-1})						
COUP	0.87	0.32	0.79	0.10	0.37	444
TESSEL	0.86	0.21	0.71	−0.09	0.39	444
TESSEL*	0.86	0.25	0.87	0.11	0.37	444

TABLE 5. Accumulated evaporation components in the Norunda forest, 16 May–31 Oct 1995. TESSEL* is the modified version adopted to the Norunda site, including seasonal variation in leaf area index and reduction of minimum canopy resistance for high vegetation to 75% of its original value.

Source	Total (mm)	Soil (mm)	Transpiration (mm)	Interception (mm)	Interception (% of precipitation)
COUP	321	45	209	67	26
TESSEL	273	48	172	54	21
TESSEL*	308	43	210	55	22
Observations (Grelle et al. 1997)	322[a]	56[b]	243[c]	74[d]	30

[a] Eddy correlation.
[b] Forest floor evaporation.
[c] Sap flow.
[d] Residual of precipitation and throughfall observations.

small. The accumulated evapotranspiration during November–December 1994–95, and January–March 1995–96, was 51, 47 (48), and 54 mm, as estimated by the COUP model, the TESSEL (TESSEL*) model, and the eddy-correlation observations, respectively. Nevertheless, the two different model strategies for representing forest snow evaporation did result in different interannual variations. The explicit representation of snow interception in COUP gave more evaporation during mild and wet winters, when the potential evaporation is typically higher compared to cold winters like that of 1995–96. The maximum simulated evaporation from intercepted snow with the COUP model was 0.16 mm h^{-1} (maximum daily average was 0.6 mm day^{-1}), which is still lower than the 0.3 mm h^{-1} reported by Lundberg and Halldin (1994) for a Swedish forest. Lundberg et al. (1998) also found evaporation rates from intercepted snow as high as 0.56 mm h^{-1} at a site in Scotland.

The observed winter sensible heat flux for the forest was well reproduced by the COUP model, whereas it was systematically overestimated by the TESSEL models (Fig. 2a). Gustafsson et al. (2003) argued that the underestimation of downward sensible heat flux by the TESSEL model was due to an erroneous ratio between the aerodynamic coupling and the thermal conductivity in the soil surface. The conclusion was that too much heat was taken from the soil instead of from the air to balance the negative net radiation. This is further supported by our results with the COUP model, in which an upper limit (500 s m^{-1}) for the aerodynamic resistance was used to avoid unrealistic cooling of the canopy. This clearly resulted in a much better agreement with observed sensible heat fluxes.

Simulated and observed net radiation agreed well in general. The slight underestimation by the COUP model (Tables 3 and 4) is related to the fact that the COUP model simulated higher downward sensible heat fluxes and thereby higher surface temperatures. On the other hand, observed forest soil temperatures were well reproduced by the COUP model (Fig. 3a), whereas the annual amplitude was greatly overestimated by the TESSEL model. The thermal conductivity of the soil surface had to be reduced to 90% of its default value in the TESSEL model, to reproduce the observed soil temperatures (Gustafsson et al. 2003). This corresponded well with the parameterization used in the COUP model.

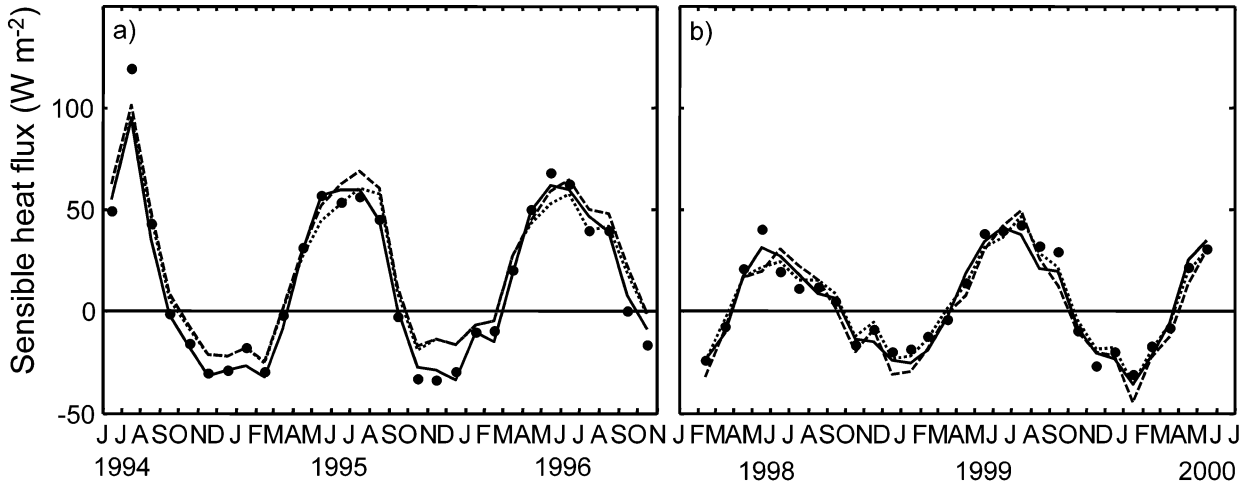

FIG. 2. Sensible heat flux for (a) Norunda forest 1994–96 and (b) Marsta arable land 1997–2000, monthly averages, measurements (crosses), and simulations with the COUP (solid line), the TESSEL (dashed line), and the TESSEL* (dotted line) models.

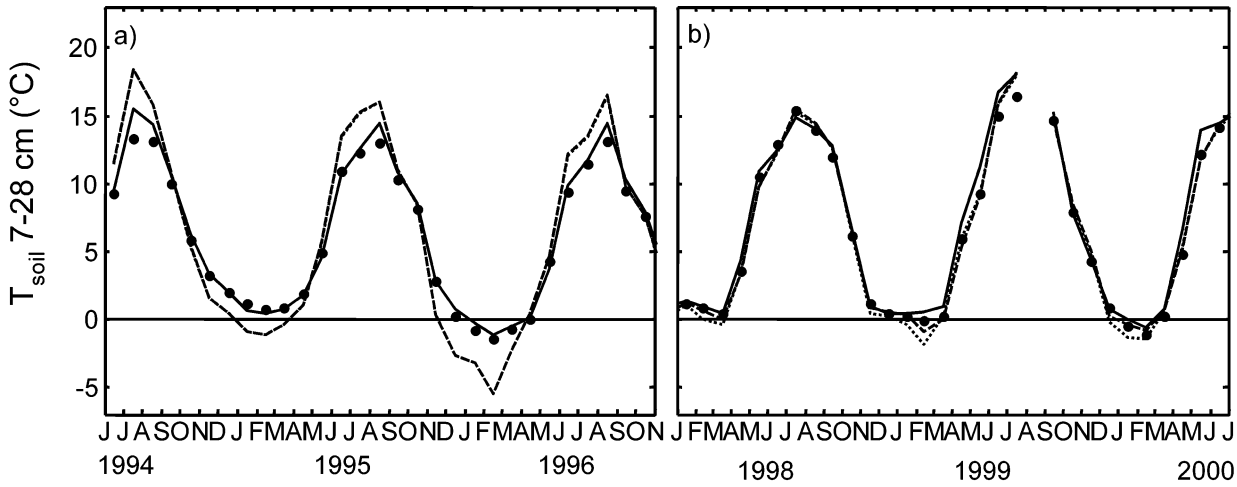

FIG. 3. Soil temperature at 7–28-cm depth for (a) Norunda forest 1994–96 and (b) Marsta arable land 1997–2000, monthly averages, measurements (crosses), and simulations with the COUP (solid line), the TESSEL (dashed line), and the TESSEL* (identical to TESSEL) models.

However, a reduced thermal conductivity between the vegetation and the soil induced an unrealistic surface cooling during stable conditions, due to the large stability correction of aerodynamic resistances. This was avoided in the COUP model as described above. A correct surface energy balance is of highest priority for the TESSEL model. Therefore, the errors in simulated soil temperatures were tolerated. The increase in soil temperatures in spring was well simulated by both models, which indicates that the simulation of the snow cover was reasonable. Unfortunately, observations of snow cover in the Norunda forest were lacking.

The observed variation in soil water storage was reasonably well reproduced by the COUP model (Fig. 4a). Discrepancies could be attributed to the large spatial variation in the observations caused by substantial soil heterogeneity. The more site-specific parameter values in the COUP model resulted in a better agreement with observations than for the TESSEL model. The models differed with respect to soil freezing in winter and the depth distribution of water uptake in summer.

2) MARSTA ARABLE LAND, 1997–2000

Statistics of the comparison between simulated and observed variables for the Marsta site are presented in Tables 6 and 7, for the warm and cold seasons, respectively. Generally, the observed sensible heat flux and the temporal variation in latent heat flux (only included as a reference for the seasonal pattern because of the systematic underestimation in the measurements) were well reproduced by all models (Figs. 1b and 2b). The

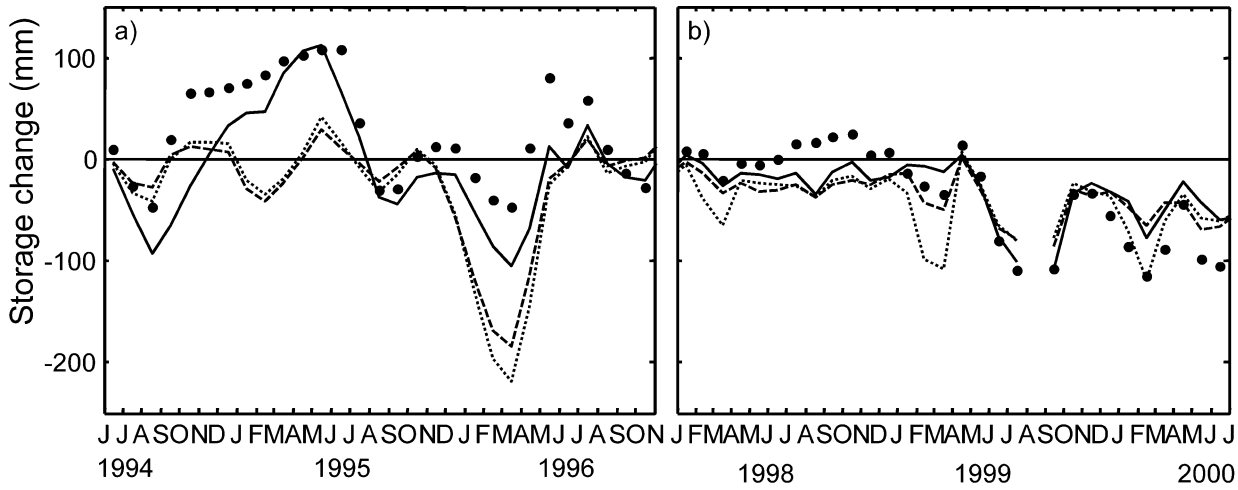

FIG. 4. Change in soil water storage in the top 100 cm for (a) Norunda forest 1994–96 and (b) Marsta arable land 1997–2000, monthly averages, measurements (crosses), and simulations with the COUP (solid line), the TESSEL (dashed line), and the TESSEL* (dotted line) models.

TABLE 6. Simulated values vs observations, summer days (May–Oct) for Marsta site 1997–2000, based on daily averages. TESSEL* is the modified version adopted to the Marsta site, including seasonal variation in LAI, vegetation cover, and roughness length.

Variable	r^2	a_0	a_1	ME	Rmse	N
LE (W m^{-2})						
COUP	0.63	19.13	1.16	24.81	32.42	211
TESSEL	0.76	18.63	1.19	25.25	29.89	211
TESSEL*	0.79	12.42	1.37	25.49	31.55	211
H (W m^{-2})						
COUP	0.79	1.71	0.86	−1.42	11.53	272
TESSEL	0.62	3.93	0.80	−0.34	16.03	272
TESSEL*	0.65	5.55	0.72	−0.54	14.61	272
R_n (W m^{-2})						
COUP	0.98	−4.89	1.04	−1.76	7.36	435
TESSEL	1.00	−3.60	1.07	1.87	5.40	435
TESSEL*	0.99	−4.35	1.07	1.78	5.88	435
T 7–21 cm (°C)						
COUP	0.90	0.75	0.99	0.59	1.24	385
TESSEL	0.96	−0.26	1.04	0.19	0.77	385
TESSEL*	0.96	−0.31	1.04	0.12	0.72	385

results were somewhat better for the COUP and the TESSEL* models when compared with the original TESSEL model (Figs. 1b and 2b). Although discrepancies between models were relatively small in general, some systematic differences in model to observation agreements were identified.

The observed summer sensible heat flux was better reproduced by the COUP model compared to the TESSEL models (Table 6). Introducing a seasonal variation in vegetation properties in TESSEL* only slightly improved the simulation of sensible heat flux in summer (Fig. 2b and Table 6), because the reduction in transpiration was compensated for by increased evaporation from bare soil.

Downward sensible heat flux during winter was overestimated by the TESSEL model in comparison with the observations when using a constant roughness length of 0.1 m throughout the year (Fig. 2b). The results improved significantly when the roughness length over snow-covered areas was reduced by one order of magnitude (Table 7), and were then even slightly better than those of the COUP model.

Simulated net radiation compared well to observations for all models during the whole period (Tables 6

TABLE 7. Simulated values vs observations, winter days (Nov–Apr) for Marsta site 1997–2000, based on daily averages. TESSEL* is the modified version adopted to the Marsta site, including seasonal variation in LAI, vegetation cover, and roughness length.

Variable	r^2	a_0	a_1	ME	Rmse	N
LE (W m^{-2})						
COUP	0.40	4.06	0.81	2.69	13.14	274
TESSEL	0.69	6.43	1.28	8.50	14.33	274
TESSEL*	0.75	2.99	1.16	4.16	9.64	274
H (W m^{-2})						
COUP	0.81	−1.72	1.02	−1.89	10.99	323
TESSEL	0.72	−4.39	1.07	−5.18	15.75	323
TESSEL*	0.84	0.07	0.99	0.15	9.54	323
R_n (W m^{-2})						
COUP	0.95	−1.88	0.93	−2.30	8.06	532
TESSEL	0.98	−1.53	1.05	−1.24	5.43	532
TESSEL*	0.98	−1.25	1.00	−1.26	4.90	532
T 7–21 cm (°C)						
COUP	0.92	0.28	1.09	0.41	0.89	512
TESSEL	0.92	−0.12	1.03	−0.08	0.75	512
TESSEL*	0.88	−0.59	1.16	−0.37	1.13	512
Albedo (−)						
COUP	0.78	0.04	0.97	0.02	0.12	521
TESSEL	0.62	0.10	0.58	−0.07	0.16	521
TESSEL*	0.65	0.09	0.67	−0.04	0.14	521

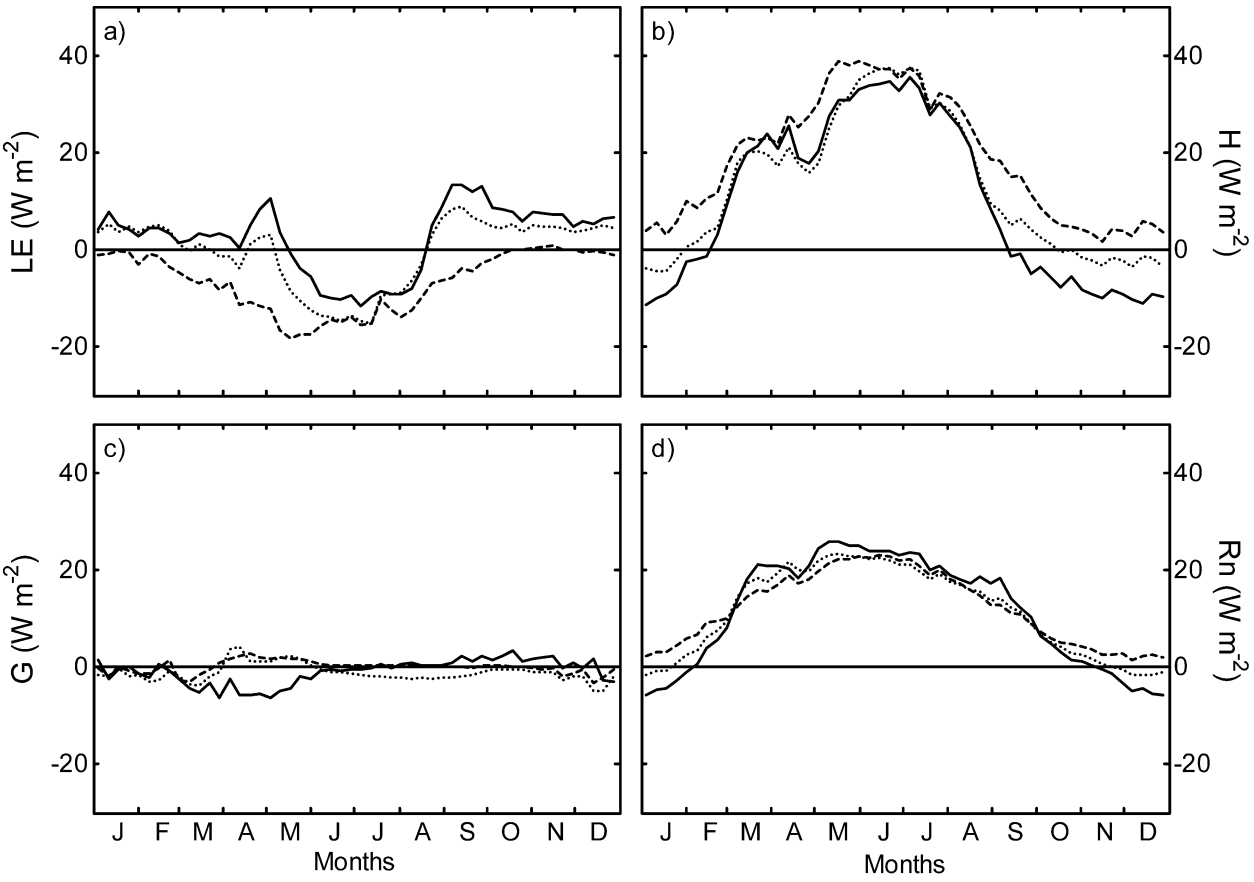

FIG. 5. Annual cycles of the discrepancy between forest and arable land in (a) latent heat flux, (b) sensible heat flux, (c) ground heat flux, and (d) net radiation, simulations with the COUP (solid line with markers) and the TESSEL models (operational: dashed line; modified: dotted line) using the Marsta dataset 1975–99.

and 7). However, as for the forest site the COUP model slightly underestimated the net radiation in comparison with the measurements, which indicates that the contribution of sensible heat flux to the surface energy balance might have been overestimated. On average, the COUP model underestimated the sensible heat flux, but the discrepancies lay within the range of the expected measurement error.

Soil temperatures were simulated with similar accuracy by all models. However, winter soil temperatures simulated by the TESSEL models were 1°–3°C lower than those predicted by the COUP model (Fig. 3b), because of differences in the simulated snow cover depth and the parameterization of the soil freezing characteristic curve. The COUP model systematically estimated a deeper snowpack, which resulted in a more effective thermal insulation of the soil. The reduced downward sensible heat flux over snow in the tuned TESSEL model (TESSEL*) further increased the cooling of the soil in comparison with the operational model (Fig. 3b).

Observed surface winter albedo was best reproduced by the COUP model, probably because of a better parameterization of snow albedo and a slightly better simulation of the snow cover evolution ($r^2 = 0.54$ and $a_1 = 0.83$ for COUP, and $r^2 = 0.60$ and $a_1 = 0.53$ for TESSEL*).

The pattern of variation in soil water storage was reasonably well reproduced by all models. As for the forest, discrepancies can be related to the limited representativity of spatially variable small-scale measurements for field-scale soil moisture conditions. Differences between models were due to differences in parameterization of soil properties.

b. 30-yr simulations: Forest versus arable land

1) LATENT HEAT FLUX AND EVAPORATION COMPONENTS

The seasonal pattern in latent heat flux from forest and arable land differed significantly according to the COUP model simulations (Fig. 5a). The latent heat flux from the forest was higher than from the arable land during winter, spring, and autumn, whereas it was higher from the arable land in the middle of the summer. This is explained by differences in transpiration and soil evaporation as controlled by LAI, canopy surface resistance, and radiation (Figs. 6a and 6b), the more con-

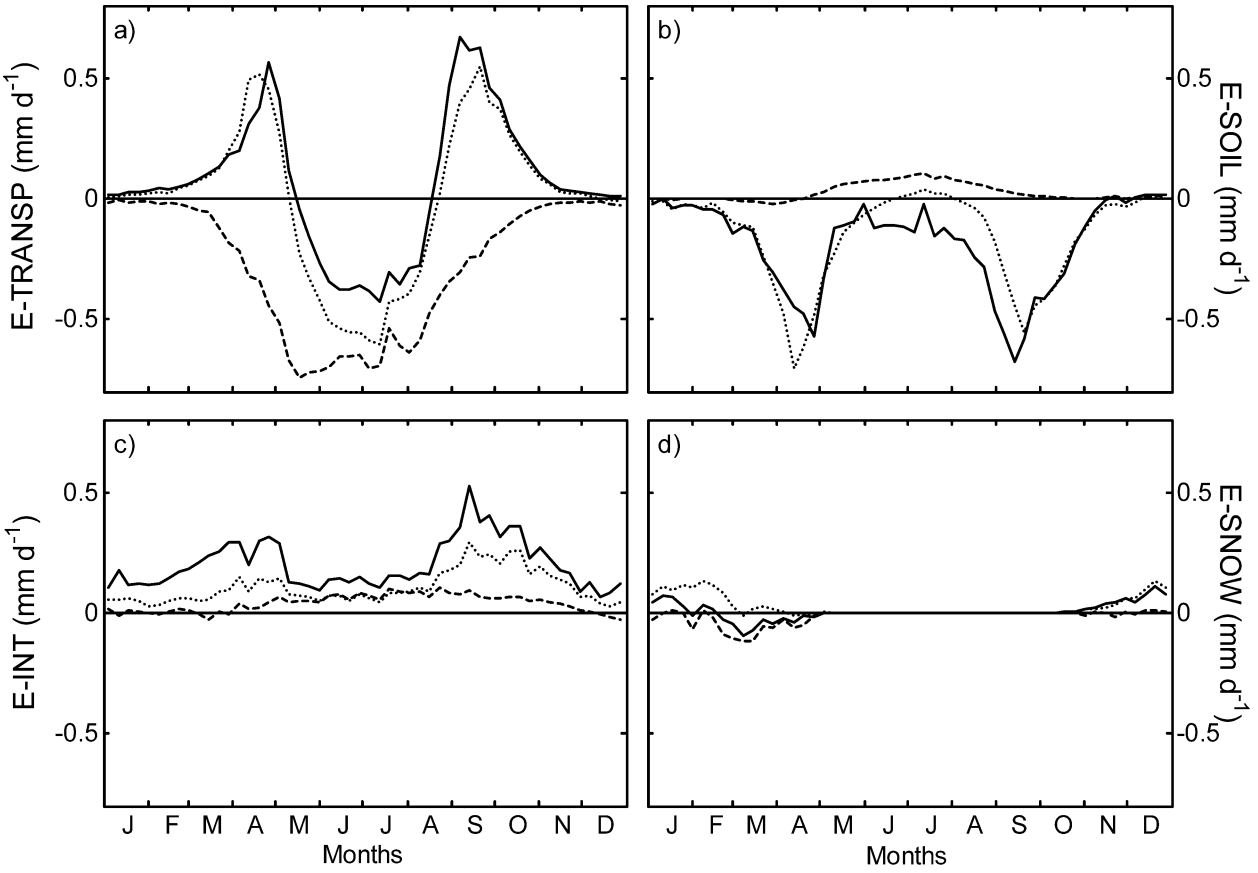

FIG. 6. Annual cycles of the discrepancy between forest and arable land in evaporation components from (a) transpiration, (b) bare soil, (c) intercepted water, and (d) snow, simulations with the COUP (solid line with markers) and the TESSEL models (operational. dashed line; modified: dotted line) using the Marsta dataset 1975–99.

servative water use by the forest trees, and the higher evaporation of intercepted water from the forest (Fig. 6c) as controlled by lower aerodynamic resistances and higher interception storage when compared with arable land.

Generally, the transpiration in the forest started in March–April, and reached its maximum rate already in June. The transpiration from the arable land started later, but increased rapidly following the evolution of LAI. The maximum rates in July exceeded the forest transpiration by about 0.5 mm day^{-1} averaged over a 7-day period, whereas the reverse was obtained in April and September (Fig. 6a). Soil evaporation showed an opposite pattern. Simulated soil evaporation from arable land exceeded that from the forest during snow-free conditions in spring and autumn (Fig. 6b). This nearly compensated for the differences between the systems with regard to transpiration. However, the evaporation of intercepted water was higher from the forest than from the arable land at all times of the year (Fig. 6c), and the difference was systematically larger during winter when the interception storage was relatively small on the arable land.

Differences in seasonal patterns between the COUP and the TESSEL simulations were mainly attributed to the different treatment of snow and interception evaporation during winter and the lower and static leaf-area index for open arable land in TESSEL. The introduction of a seasonal variation in leaf-area index for both land covers significantly reduced the systematic differences between the models, especially with respect to arable land. However, the lack of interception evaporation during winter in the TESSEL model remained as a major cause of discrepancy in the seasonal patterns reproduced by the two models (Fig. 6c).

2) SENSIBLE HEAT FLUX

The sensible heat flux from the forest greatly exceeded that from the arable land in summer (Fig. 5b). This was primarily caused by the higher canopy surface resistance of the forest compared to the arable crop, which controlled the rate of transpiration and, consequently, the latent heat flux. Second, it was a result of the higher net radiation and the lower aerodynamic resistance of the forest. Typically, negative sensible heat fluxes in the middle of the day due to the high evapo-

transpiration from the fields were observed at Marsta in summer.

The winter was characterized by the large downward sensible heat flux over both forest and arable land. The downward sensible heat flux over the forest exceeded that for arable land during November–December, which corresponded to the larger net loss of latent heat from the forest during these periods. However, the average sensible heat flux over the forest increased to positive (upward) values already in March, following the annual course of net radiation; whereas it remained negative (downward) over the arable land throughout March and April. It is, thus, reasonable to assume that in a patchy landscape like the NOPEX region, the forest contributes sensible heat to the snowmelt in open areas. The seasonal differences between forest and open land were more pronounced in the COUP simulations due to the higher losses of latent heat by interception evaporation in winter, which were not accounted for in the TESSEL models.

3) NET RADIATION

The net radiation was generally higher above the forest compared to the arable field (Fig. 5d), due to the lower albedo of the forest at all times of the year. The albedo of the forest was only 8% in summer and did not exceed 20% in winter. The albedo of the arable land was up to 60% in winter, and was never below 20% in summer. However, because the global radiation was relatively low during the main part of the winter, the large discrepancy in albedo was of minor importance for the net radiation from November to February. The largest difference in net radiation between forest and arable land (about 20 W m^{-2}) occurred from the final snowmelt in April throughout the vegetation season (Fig. 5d).

4) SOIL TEMPERATURE AND SNOW DEPTH

The simulated soil temperatures showed typical differences between the forest and the arable land. The annual amplitude was 2°–7°C larger in the arable land than in the forest in the top 7 cm of the soil, and 2°–4°C larger in the 28–100-cm layer. This was due to the lower thermal conductivity in the topsoil, the larger fraction of net radiation absorbed by the canopy and the reduced turbulent exchange from the forest floor compared to the arable land (Table 2). The seasonal differences between the two surface types were, however, less pronounced in the simulations with the TESSEL model, due to the exaggerated thermal coupling between the soil and the canopy in the forest as previously discussed.

The maximum simulated snow depth was about 20 cm both in the forest and on the arable land. The largest difference (about 8 cm or 20%–30% more in the forest) occurred toward the end of the snowmelt season. The final snowmelt was delayed about 10 days in the forest in comparison with open land, which can be expected because of the reduced radiation below the canopy (Ohta et al. 1993). Less accumulation of snow might be expected in the forest because of evaporation of intercepted snow (Harding and Pomeroy 1996). However, higher inputs of sensible and latent heat fluxes to the snowpack in open areas can compensate for these differences in a Seandinavian climate characterized by several snowmelt events throughout the winter (Koivusalo and Kokkonen 2002).

5) ANNUAL WATER AND HEAT BALANCE

The accumulated net radiation was 1216–1296 for forest and only 856–934 MJ m^{-2} yr^{-1} for the arable land (Fig. 7). In other words, the forest absorbed about 40% more radiation than the arable land, mainly because of its lower albedo at all times of the year. The partitioning of net radiation into latent heat flux and sensible heat flux differed significantly between the forest and the arable land. The average Bowen ratio (H/LE) for the forest was approximately 0.9 (1.7 midday) in July based on the COUP model simulations, whereas the corresponding figure for the arable land was 0.3 (0.6 midday). These results are comparable to those reported by Bringfelt et al. (1999). The large difference in net radiation between the two surface types was mainly balanced by the sensible heat fluxes, because the difference in latent heat flux was much smaller (Fig. 7). The arable land was a net sink for sensible heat, due to large negative winter sensible heat fluxes used for snowmelt and the high rates of evaporation during summer. However, during the calibration period the accumulated measured sensible heat flux was positive and constituted 11% and 25% of the net radiation in the open land and the forest, respectively. This could most likely be explained by slightly different average climate conditions in comparison with the 30-yr period. The forest calibration period (1994–96) was drier (18% less precipitation in both summer and winter), while the arable land dataset (1997–2000) was characterized by warmer and more humid winters (1° higher average air temperature from November to April). The annual heat budgets based on the TESSEL models differed from those by the COUP model mainly because of smaller downward sensible heat flux in winter and the lack of evaporation from intercepted snow in the TESSEL model. For arable land, the introduction of seasonal variation in leaf-area index (TESSEL*) influenced the within-year distribution of latent heat flux (Fig. 6a) and the partitioning into different evaporation components as well as the total annual flux (Fig. 7). For the forest, sensible heat flux was significantly reduced in the ''tuned'' TESSEL model (Fig. 7), mainly because of the increased summer evaporation.

The net heat storage in the ground could be expected to be around zero, when averaged over several years. The results presented in Fig. 7 indicate considerable net heat storage in the ground. However, the ground heat

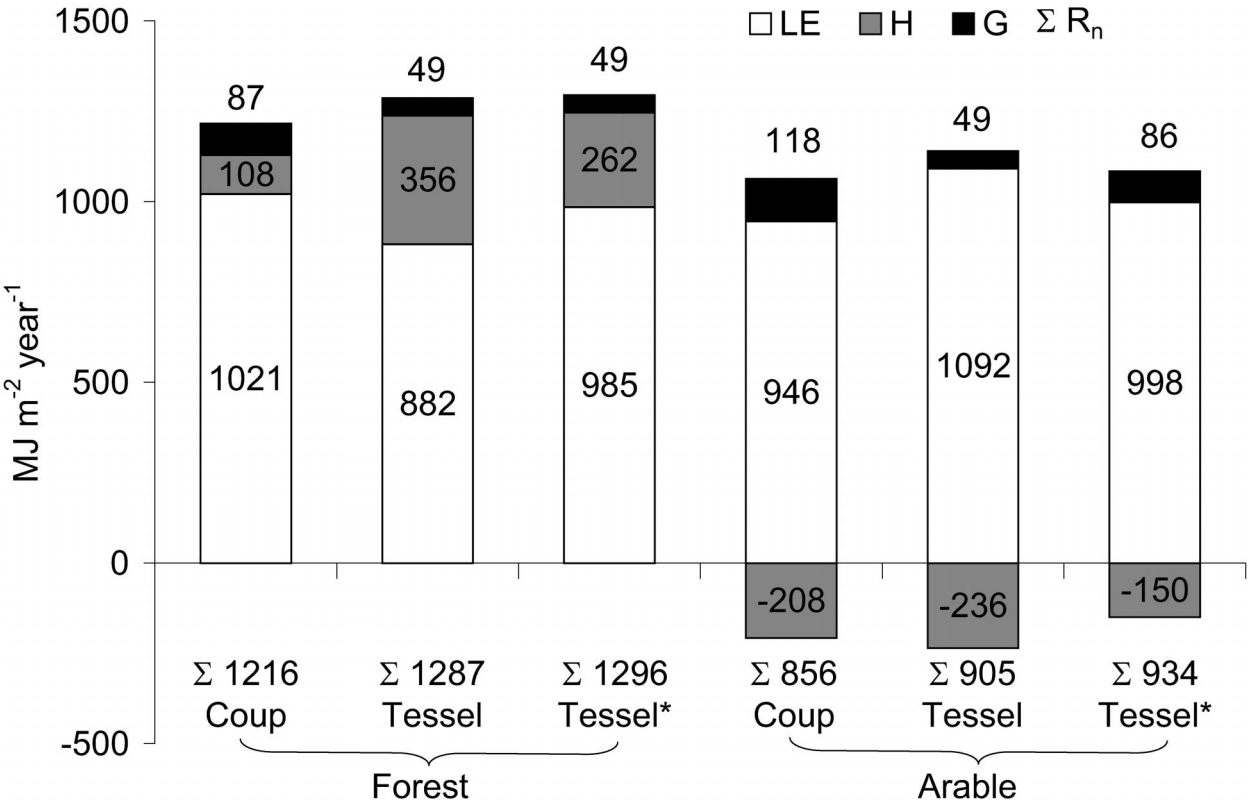

FIG. 7. Average annual heat budget for forest and arable land, simulated with the COUP, the TESSEL, and the modified TESSEL* models using the Marsta dataset 1975–99.

flux in this context also includes the energy needed to melt the snowpack in spring. The average cumulative snowfall was 138 mm yr^{-1}, which corresponds to a latent heat flux of -46 MJ m^{-2} yr^{-1}.

The annual totals of different evaporation components based on the COUP model confirm the general pattern that differences between forest and arable land were mainly attributable to higher interception evaporation from the forest, which was partly counteracted by higher evaporation from bare soil in arable land (Fig. 8). However, this pattern was not distinguished in the TESSEL simulations for which evaporation from intercepted snow was not accounted. The original TESSEL model also showed proportionally less soil evaporation and more transpiration from arable land because of the use of a static leaf-area index. The partitioning into different evaporation components for arable land as well as annual forest transpiration was much closer to the COUP model when a seasonal variation in LAI and a more representative value for the forest minimum canopy resistance were used.

4. Concluding remarks

Simulations with a detailed SVAT model (COUP) and a ''tuned'' version of a GCM land surface scheme (TESSEL*) agreed well with observed values of energy balance components and soil temperatures during a 3-yr period for the forest, as well as for arable land. Results from the GCM land surface scheme parameterized with operational values (TESSEL) differed from the observations for both types of land covers in some important aspects. The introduction of seasonal variations in leaf-area index and tuning of canopy surface resistance reduced the discrepancies with observations for both forest and arable land. A reduction of the roughness length over snow-covered open land also significantly improved the accuracy of simulations for arable ''open land.'' These modifications reduced the simulated latent heat flux in winter, spring, and autumn and also improved the simulation of sensible heat. Although models differed in several model concepts and parameter values the tuned GCM scheme (TESSEL*) then reproduced observations with similar accuracy as the COUP model. The results differed systematically in some aspects, but except for sensible heat flux in winter, the overall performance of these two models was equally good with respect to surface energy balance components, considering the uncertainties in observations and energy balance closure.

The forest sensible heat flux was best reproduced by the detailed SVAT model, whereas the latent heat flux was better reproduced by the tuned GCM scheme. However, latent heat flux was difficult to reproduce well for

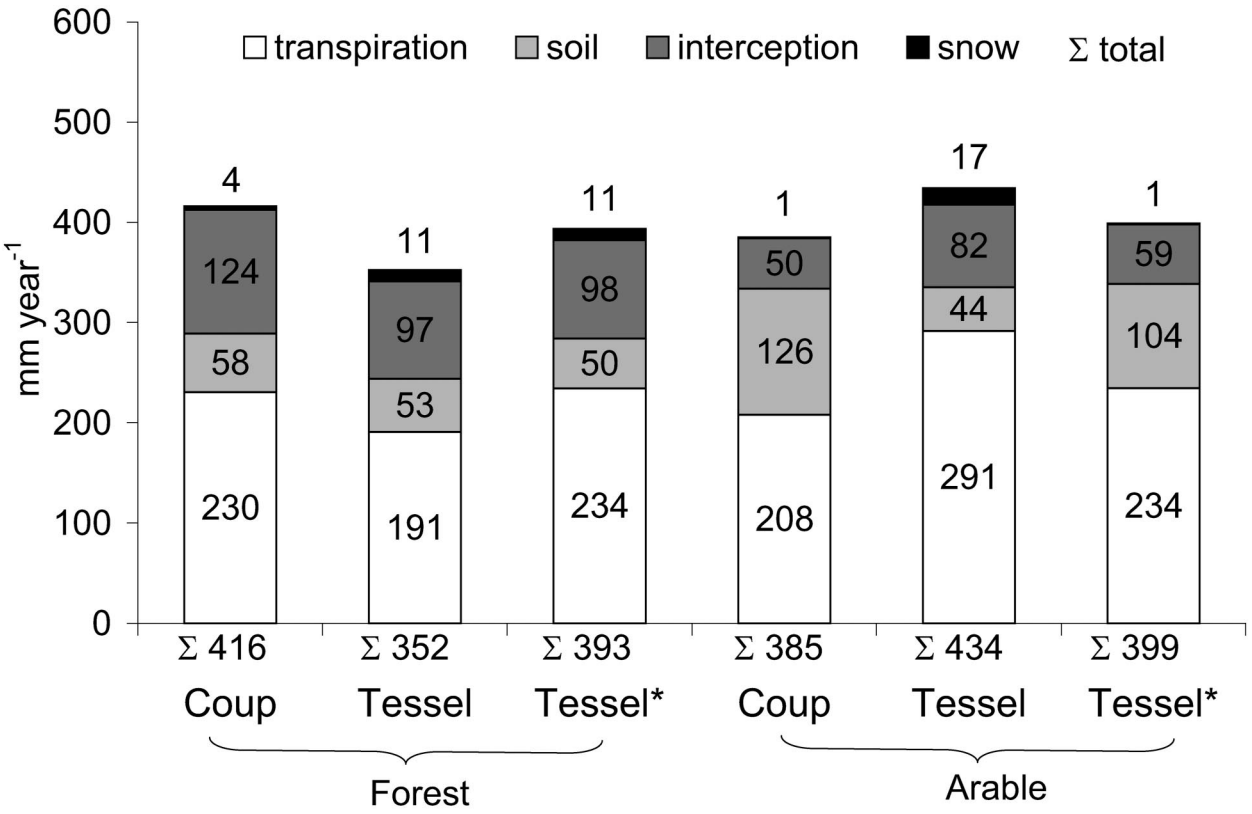

FIG. 8. Average annual evapotranspiration and its components for forest and arable land, simulated with the COUP, the TESSEL, and the modified TESSEL* models using the Marsta dataset 1975–99; transpiration (white), soil evaporation (light gray), evaporation of intercepted water (dark gray), and snow evaporation (black).

all years, probably because of interannual variations in vegetation properties that were not accounted for in the models. The winter sensible heat flux from the forest was systematically overestimated by the GCM scheme in comparison with the observations, whereas it was well reproduced by the detailed SVAT model.

Based on the 30-yr simulations, the accumulated net radiation was 40% higher in the forest when compared with the arable land. The forest was a net source of sensible heat flux, whereas the arable land was a net sink. Transpiration was higher from arable land in summer, and total soil evaporation exceeded that from the forest, whereas interception evaporation was higher from the forest at all times of the year.

The average seasonal patterns and differences in energy fluxes of the two types of land cover over the 30-yr period obtained with the detailed SVAT model were better reproduced by the tuned version of the GCM land surface scheme than by the operational version. This demonstrates the robustness of the simple modifications to the GCM land surface scheme and the significant importance of including seasonal dynamics in vegetation properties to represent forest and open land within the boreal zone with a reasonable accuracy in GCM types of SVAT schemes.

However, the restriction of interception evaporation to snow-free conditions in the GCM model remained as a source of considerable discrepancy between the two types of models. As a consequence, total annual latent heat flux from the forest exceeded that from the arable land as predicted by the detailed SVAT model, whereas the ''tuned'' GCM model showed no difference between the two surface types. This demonstrates the importance of accounting for evaporation from intercepted snow to adequately represent land surface energy fluxes within the boreal zone. The significance of seasonal variation in vegetation properties for simulation of global rainfall patterns was recently shown by van den Hurk et al. (2003). However, a more physically sound representation of forest snow evaporation does not necessarily have a significant impact on larger-scale climatic patterns due to the feedback from the atmosphere, as recently shown by Essery et al (2003).

The results also demonstrate that the evaluation of different model schemes includes a delicate balance between the relative importance of different model concepts, the reliability of observed data, and the choice of parameter values concerning the specific scale of consideration.

Acknowledgments. The availability of data from the Norunda and Marsta sites is gratefully acknowledged.

We sincerely thank Prof. A Lindroth (Lund University) and Dr. A. Grelle (Swedish University of Agricultural Sciences) for data on sensible and latent heat fluxes, Dr. E. Cienciala (Institute of Forest Ecosystem Research, Czech Republic) for sap flow data, Dr. M. Mölder (Lund University) for radiation and climatic data, Dr. J. Seibert (Swedish University of Agricultural Sciences) for precipitation data, and Dr. E. Kellner (Uppsala University) for data on soil temperature and soil moisture conditions from the Norunda site. Thanks are also given to Prof. S. Halldin and Dr. Hans Bergström (Uppsala University) for radiation and climatic data from the Marsta site. Meteorological data from Uppsala Airport were obtained from the Swedish Meteorological and Hydrological Institute (SMHI). We also thank Dr. P. Viterbo (ECMWF) for making the TESSEL model available and Prof. N. Jarvis for valuable comments on the manuscript. Language correction was made by Mary McAfee. This project was funded by the Swedish Research Council.

REFERENCES

Barfield, B. J., F. A. Payne, and J. N. Walker, 1973: Surface water storage of selected crop leaves under irrigation sprays. *Agric. Meteor.*, **12,** 105–111.

Bonan, G. B., F. S. Chapin, and S. L. Thomson, 1995: Boreal forest and tundra ecosystems as components of the climate system. *Climatic Change,* **29,** 145–167.

Bringfelt, B., M. Heikinheimo, N. Gustafsson, V. Perov, and A. Lindroth, 1999: A new land-surface treatment for HIRLAM—Comparisons with NOPEX measurements. *Agric. For. Meteor.*, **98–99,** 239–256.

Chen, T., and Coauthors, 1997: Cabauw experimental results from the Project for Intercomparison of Landsurface Parameterization Schemes (PILPS). *J. Climate,* **10,** 1194–1215.

Cienciala, E., J. Kucera, and A. Lindroth, 1999: Long-term measurements of stand water uptake in Swedish boreal forest. *Agric. For. Meteor.*, **98–99,** 547–554.

de Vries, D. A., 1975: Heat transfer in soils. *Transfer Processes in Plant Environment,* D. A. de Vries, and N. H. Afgan, Eds., Vol. 1, *Heat and Mass Transfer in the Biophere. I. Transfer Processes in Plant Environment,* Scripta Book, 5–28.

Douville, H., and J.-F. Royer, 1997: Influence of the temperate and boreal forests on the Northern Hemisphere climate in the Météo-France climate model. *Climate Dyn.,* **13,** 57–74.

Essery, R., J. Pomeroy, J. Parviainen, and P. Storck, 2003: Sublimation of snow from coniferous forests in a climate model. *J. Climate,* **16,** 1855–1864.

Grelle, A., 1997: Long-term water and carbon dioxide fluxes from a boreal forest: Methods and applications. Ph.D. thesis, Silvestria 28, Acta Universitaris Agriculturae Suecìae, 80 pp. [Available from Department for Production Ecology, Box 7042, S-750 07 Uppsala, Sweden.]

——, and A. Lindroth, 1996: Eddy-correlation system for long-term monitoring of fluxes of heat, water vapour and CO2. *Global Change Biol.*, **2,** 297–307.

——, A. Lundberg, A. Lindroth, A.-S. Moren, and E. Cienciala, 1997: Evaporation components of a boreal forest: Variations during the growing season. *J. Hydrol.,* **197,** 70–87.

——, A. Lindroth, and M. Mölder, 1999: Seasonal variation of boreal forest surface conductance and evaporation. *Agric. For. Meteor.*, **98–99,** 563–578.

Gustafsson, D., 2002: Boreal land surface water and heat balance—Modelling soil-snow-vegetation-atmosphere behaviour. Ph.D. thesis, TRITA-LWR PHD 1002, Royal Institute of Technology, 35 pp. [Available from Department of Land and Water Resources Engineering, KTH, SE-100 44, Stockholm, Sweden.]

——, M. Stähli, and P.-E. Jansson, 2001: The surface energy balance of a snow cover: Comparing measurements to two different simulation models. *Theor. Appl. Climatol.,* **70,** 81–96.

——, and Coauthors, 2003: Boreal forest surface parameterization in the ECMWF model—1D test with NOPEX long-term data. *J. Appl. Meteor.*, **42,** 95–112.

Halldin, S., 2001: Wintertime radiation budget, photometric correction of the atmosphere for satellite remote sensing and in-situ calibration of net radiometers. *Theor. Appl. Climatol.,* **70,** Documented dataset on appended CD-ROM.

——, L. Gottschalk, A. A. van den Griend, S.-E. Gryning, M. Heikinheimo, U. Högström, A. Jochum, and L.-C. Lundin, 1998: NOPEX—A Northern Hemisphere climate processes land surface experiment. *J. Hydrol.,* **212–213,** 172–187.

——, and Coauthors, 1999: Continuous long-term measurements of soil-plant-atmosphere variables at an agricultural site. *Agric. For. Meteor.,* **98–99,** 75–102.

Harding, R. J., and J. W. Pomeroy, 1996: The energy balance of the winter boreal landscape. *J. Climate,* **9,** 2778–2787.

Hedstrom, N. R., and J. W. Pomeroy, 1998: Measurements and modelling of snow interception in the boreal forest. *Hydrol. Process.,* **12,** 1611–1625.

Heidmann, T., A. Thomsen, and K. Schelde, 2000: Modelling soil water dynamics in winter wheat using different estimates of canopy development. *Ecol. Modell.,* **129,** 229–243.

Henderson-Sellers, A., 1996: Soil moisture simulation: Achievements of the RICE and PILPS intercomparison workshop and future directions. *Global Planet. Change,* **13,** 99–115.

Houghton, J. T., L. G. Meira Filho, B. A. Callender, N. Harris, A. Kattenberg, and K. Maskell, Eds., 1996: *Climate Change 1995: The Science of Climate Change.* Cambridge University Press, 572 pp.

Jansson, P.-E., and S. Halldin, 1979: Model for the annual water and energy flow in a layered soil. *Comparison of Forest and Energy Exchange Models,* S. Halldin, Ed., Society for Ecological Modelling, 145–163.

——, and L. Karlberg, 2001: *Coupled Heat and Mass Transfer Model for Soil-Plant-Atmosphere Systems.* Department of Civil and Environmental Engineering, Royal Institute of Technology, Engineering, 321 pp.

——, E. Cienciala, A. Grelle, E. Kellner, A. Lindahl, and M. Lundblad, 1999: Simulated evapotranspiration from the Norunda forest stand during the growing season of a dry year. *Agric. For. Meteor.*, **98–99,** 621–628.

——, D. Gustafsson, and M. Stähli, 2001: Continuous measurements of water and heat balance in soil, snow and atmosphere at an agricultural field in mid-Sweden, November 1997-April 1998. *Theor. Appl. Climatol.*, **70,** Documented dataset on appended CD-ROM.

Johnsson, H., and P.-E. Jansson, 1991: Water balance and soil moisture dynamics of field plots with barley and grass ley. *J. Hydrol.,* **29,** 149–173.

Kellner, E., P.-E. Jansson, A. Lindahl, M. Stähli, K. Hessel, J. Eriksson, and L.-C. Lundin, 1999: The influence of soil moisture dynamics on transpiration at the CTS pine stands. *Agric. For. Meteor.*, **98–99,** Documented dataset on appended CD-ROM.

Koivusalo, H., and T. Kokkonen, 2002: Snow processes in a forest clearing and in a coniferous forest. *J. Hydrol.,* **262,** 145–164.

Koster, R. D., and M. J. Suarez, 1992: Modeling the land surface boundary in climate models as a composite of independent vegetation stands. *J. Geophys. Res.,* **97D,** 2697–2715.

Lankreijer, H., A. Lundberg, A. Grelle, A. Lindroth, and J. Seibert, 1999: Evaporation and storage of intercepted rain analysed by comparing two models applied to a boreal forest. *Agric. For. Meteor.*, **98–99,** 594–604.

Lundberg, A., and S. Halldin, 1994: Evaporation of intercepted

snow—Analysis of governing factors. *Water Resour. Res.,* **30,** 2587–2598.

——, I. Calder, and R. Harding, 1998: Evaporation of intercepted snow: Measurement and modelling. *J. Hydrol.,* **206,** 151–163.

Lundin, L.-C., and Coauthors, 1999: Continuous long-term measurements of soil-plant-atmosphere variables at a forest site. *Agric. For. Meteor.,* **98–99,** 53–73.

Mölder, M., A. Grelle, A. Lindroth, and S. Halldin, 1999a: Flux-profile relationships over a boreal forest roughness sublayer corrections. *Agric. For. Meteor.,* **98–99,** 645–658.

——, S. Halldin, and A. Lindroth, 1999b: Characterization of the lowest 100 m of the boundary layer and the radiation budget of the surface. *Agric. For. Meteor.,* **98–99,** Documented dataset on appended CD-ROM.

Monteith, J. L., 1965: Evaporation and the atmosphere. *The State and Movement of Water in Living Organisms. 19th Symp. of the Society of Experimental Biology,* Cambridge University Press, 205–234.

Ohta, T., T. Hashimoto, and H. Ishibashi, 1993: Energy budget comparison of snowmelt rates in a deciduoud forest and an open site. *Ann. Glaciol.,* **18,** 53–59.

Penman, H. L., 1953: The physical basis of irrigation control. Vol. II, *Report of 13th Int. Horticultural Congress,* London, United Kingdom, Royal Horticultural Society, 913–924.

Persson, G., 1997: Comparison of simulated water balance for willow, spruce, grass ley and barley. *Nord. Hydrol.,* **28,** 85–98.

Sellers, P. J., and Coauthors, 1997: BOREAS in 1997: Experiment overview, scientific results, and future directions. *J. Geophys. Res.,* **102D,** 28 731–28 769.

Stähli, M., K. Hessel, J. Eriksson, and A. Lindahl, 1995: Physical and chemical description of the soil at the NOPEX central tower site. Department of Hydrology, Uppsala University NOPEX Tech. Rep. 16, 20 pp.

Thomas, G., and P. R. Rowntree, 1992: The boreal forests and climate. *Quart. J. Roy. Meteor. Soc.,* **118,** 469–497.

van den Hurk, B. J. J. M., P. Viterbo, A. C. M. Beljaars, and A. K. Betts, 2000: Offline validation of the ERA40 surface scheme. ECMWF Tech. Memo. 295, 42 pp. [Available from European Centre for Medium-Range Weather Forecasts, Shinfield Park, Reading, Berkshire, RG2 9AX, United Kingdom.]

——, and S. O. Los, 2003: Impact of leaf area index seasonality on the annual land surface evaporation in a global circulation model. *J. Geophys. Res.,* **108,** 4191, doi:10.1029/2002JD002846.

Verseghy, D. L., 2000: The Canadian Land Surface Scheme (CLASS): Its history and future. *Atmos.–Ocean,* **38,** 1–13.

Viterbo, P., and A. C. M. Beljaars, 1995: An improved land surface parameterization scheme in the ECMWF model and its validation. *J. Climate,* **8,** 2716–2748.